BOISE STATE UNIVERSITY

Computing PhD

Computational Math Science and Engineering

Comprehensive Exam Synthesis paper

Mathematical and numerical modeling of ice-ocean interface

Student
Yao Gahounzo

Advisor
Dr. Michal Kopera

Committee members

Dr. Donna Calhoun
Dr. Ellyn Enderlin
Dr. Uwe Kaiser

November 25, 2021

1 Introduction

The Antarctic and Greenland ice sheets and glaciers are important components of the global climate system. Over the past decades, the anthropogenic forces due to human activities have caused the atmosphere and the ocean to warm(Noble et al., 2020); as a result, it leads to mass loss in the global ice sheets, glaciers, and sea ice. According to Straneo and Heimbach (2013), the mass loss from the Greenland ice sheets quadrupled over the past two decades, contributing to the observed global sea-level rise about of one quarter. Observations now indicate that the impact of the Greenland ice sheet mass loss goes beyond sea-level rise to include changes in ocean properties and circulation, nutrient and sediment transport, and the ecosystem (Catania et al., 2020). Straneo and Heimbach (2013) found that the Greenland ice loss contribution to the sea level is twice that from the Antarctic ice sheets; this ice loss increased due to both increased surface melting and ice or glaciers discharge to the ocean. The latter is attributed to the acceleration of ice flow and thinning of fast-flowing marine-terminating outlet glaciers (Nick et al., 2013). Although outlet glaciers extend far into the ice sheet's interior, much work has focused on the terminal boundary at the ocean, as this is where changes in mass balance have been most significant. The widespread changes in surface melt and ice flow indicate a response to external forcings and are consistent with observations of atmospheric and oceanic warming over and around Greenland (Bersch et al., 2007; Box et al., 2009; Straneo and Heimbach, 2013). Changes in precipitation and increasing air temperatures are the external forcings that have led to increased surface melting of the ice sheet (van den Broeke et al., 2009; Straneo and Heimbach, 2013). However, the processes behind the increased ice discharge remain elusive. Glacier acceleration resulted from initial retreat of marine termini, which decreased ice flow resistance, increased calving and thinning (Nick et al., 2009; Straneo et al., 2013). The central hypothesis supporting initial glacier retreat involves increased submarine melting of the ice-ocean interface (Straneo et al., 2013). Ocean-related reduction of Greenland glacier calving faces has been observed over the past two decades (e.g., Rignot et al. (2010); Straneo and Cenedese (2015); Schaffer et al. (2017)). Progress has been made through field observations, modeling, and theoretical studies to understand the mechanisms of ice-ocean interaction and examine the plausibility of the hypothesis. However, the question regarding the submarine melting remains, as the field observation are limited.

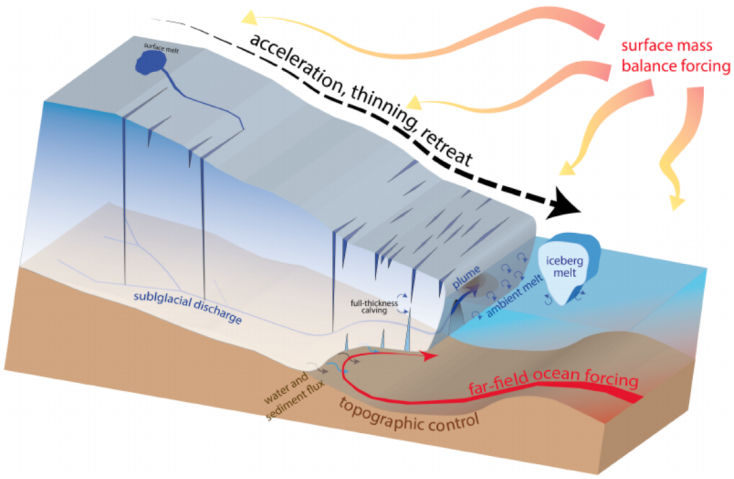

Figure 1: Source Catania et al. (2020). Conceptual diagram of outlet glacier processes that play in the terminal zone where the atmosphere, ice sheet, bedding and ocean interact. The red arrow indicates ocean thermal forcing occurring at depth in the fjords. The black arrow indicates that dynamic changes in outlet glaciers are more pronounced toward the end of the glacier. The blue arrows indicate subglacial water, which rises at the submarine terminus and rises along the end face, carrying sediment and nutrients with it (brown arrows). Subglacial plumes, melting icebergs, and distant ocean circulation all influence the circulation in the fjords (Catania et al., 2020).

According to (Jenkins, 2011), the region where the interaction between the ice and ocean occurs might include the basal and front of a floating extension of the grounded ice. Different authors have done considerable research to understand some of the processes in ice-ocean interaction, basal melting. Jenkins (2011) studied the convection-driven melting near the grounding lines of ice shelves and tidewater glaciers. The focus of their work was on the plumes generated by the meltwater from the ice shelves. Kerr and McConnochie (2015), and Gayen et al. (2016) worked on the convection at the vertical ice face dissolving where the focus was on the buoyancy-controlled dissolving. Gayen et al. (2016) solved the Navier-Stokes equations for turbulent flow at a vertical ice-ocean interface at a scale similar to that obtained in the laboratory using Direct Numerical Simulations. They found good agreement with Kerr and McConnochie (2015) experiments, consistent with buoyancy controlling the width of the interfacial sublayer. The basal ice melting is a significant component of mass loss from the Antarctic ice sheet (pri; Malyarenko et al., 2020). However, projections of Antarctic contributions under future warming global and regional climate scenarios have significantly higher uncertainty due to poorly understood processes that could lead to rapid ice melting or discharge (Weertman, 1974; DeConto and Pollard, 2016; Gwyther et al., 2020). Therefore, more studies have to be done to understand basal melting better, address the uncertainty in current contributions, and improve future projections of Antarctic contributions.

Jenkins (2011) emphasized that most melting estimates near the ice shelf grounding line have been based on observations of ice flux. Also, on the assumption of a steady-state, calculated melting or freezing and known surface ablation or accumulation balance the convergence or divergence of ice flux. Results suggest melt rates ranging from a few meters to a few tens of meters per year, with peaks either at the grounding line or a short distance downstream (Jenkins and Doake, 1991; Rignot and Jacobs, 2002; Jenkins, 2011). Melting of the vertical calving in front of a tidewater glacier is more challenging to observe; however, the net supply of meltwater to the ocean from observations of water properties in the fjord in front of LeConte Glacier front was melting at over 10 m per day (Motyka et al., 2003). Ocean circulation models under ice shelves can capture the large-scale characteristics of buoyancy-driven overturning circulation and reproduce the observed distribution of melting and freezing under ice shelves (Jenkins and Holland, 2002; Jenkins, 2011). However, the resolution of all processes operating at the grounding line is generally beyond the capabilities of most ocean circulation models.

2 Plume dynamics

Much of the meltwater from the ice sheets, glaciers, ice caps are discharged directly into the ocean at depth, generating buoyant plumes that move up the ice-ocean interface and merge with the surrounding ocean water (Hewitt, 2020). The dynamics of these plumes are essential in regulating the heat transfer that drives submarine melt and controlling the depth to which glacial meltwater is exported to the open ocean. Therefore, they are crucial in the ice sheet response to ocean warming (Joughin et al., 2012; Hewitt, 2020) and the ocean response to ice sheet melt (Straneo and Heimbach, 2013).

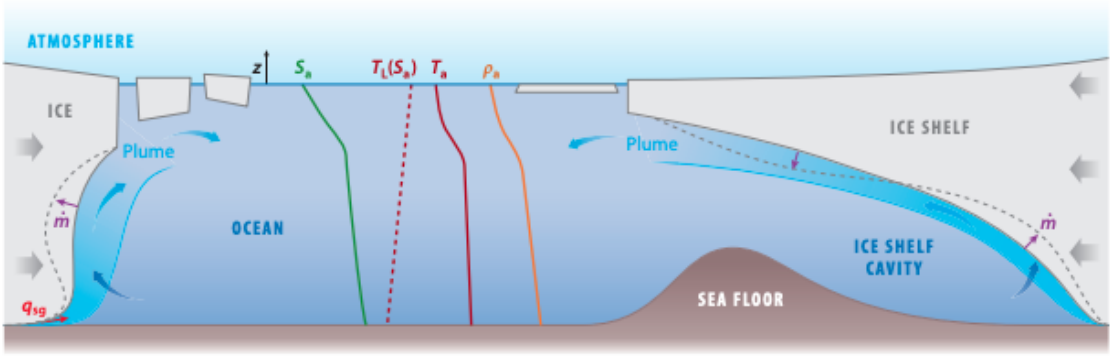

Figure 2: Source Hewitt (2020). Plumes occur at the front of tidewater glaciers and beneath floating ice shelves. Subglacial discharge q_{sg} (red arrow) and submarine melting $\dot{m}$ (purple arrows) produce buoyant water that rises up the ice front, entraining warmer ocean water. Typical profiles of ambient salinity S_a $[psu]$, temperature T_a $[°C]$, and density ρ_a $[kgm^{-3}]$, as well as liquidus $T_L(S_a)$ $[°C]$, are shown. The plume controls the melt rate and hence the shape of the ice–ocean interface. It can reach a level of neutral buoyancy and separate from the ice front, controlling the depth at which glacially modified water is exported to the open ocean (Hewitt, 2020).

As depicted in Figure 2, the plumes form at the near-vertical front of tidewater glaciers and beneath relatively low-slope ice shelves. The former is typical of Greenland, while the latter is typical of the Antarctic ice sheet. According to Hewitt (2020), tidewater glaciers, melting driven by plumes affects the shape of the front; thus plays an essential role in the calving of icebergs. Under ice shelves, melting and freezing affect the shape of the ice shelf, which significantly affects the location of the grounded line.

Seawater in the vicinity of the ice is within a few degrees of the freezing point and is a mixture of water of different origins and properties. A common assumption is that the only source of buoyancy that acts to stratify the water column and drive the overturning circulation in the ice cavity is the generation of meltwater at the ice-seawater interface (Jenkins, 2011). However, in a critical region such as Greenland, where outlet glaciers are grounded several hundred meters below sea level and terminate in a narrow fjord, freshwater will flow across the grounding line from the glacier bed. In Greenland, there are no direct observations of glaciers. However, theory and models indicate that the boundary layer is dominated by buoyant plumes driven by freshwater release from the surface melt at the ice sheet's base and from grounding line melt along the glacier face (Jenkins, 2011; Straneo and Heimbach, 2013). For that reason, accurate mathematical representation of the ice-ocean boundary is crucial for understanding the key processes of the ice-ocean interaction and the impact of Greenland and Antarctic ice loss on sea-level rise.

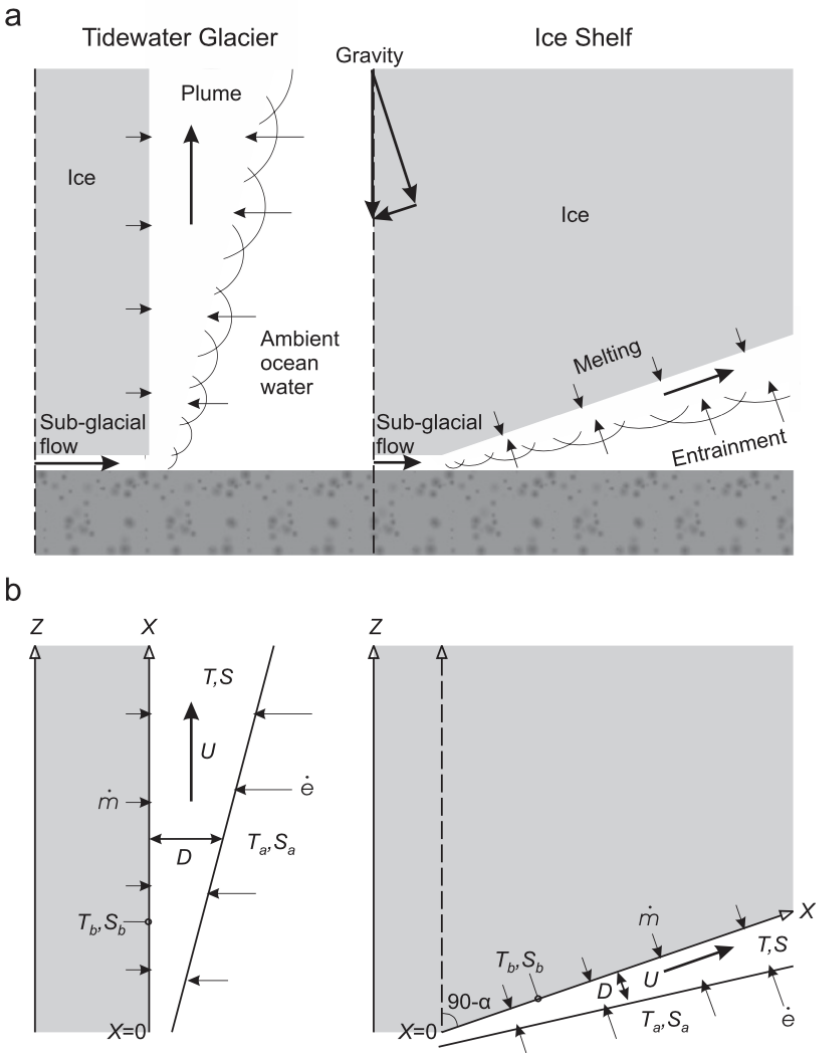

Figure 3: Source Jenkins (2011). (a) Conceptual representation of a buoyant plume from freshwater flow at the grounding line of an ice shelf or tidewater glacier and (b) schematic picture of the numerical representation of (a) with the key variables defined. The plume rises on the ice face, entraining seawater in its way. The entrained seawater provides the heat that drives the melting of the ice face, and the meltwater thus derived adds to the buoyancy of the plume. Near the grounding line, most of the freshwater carried in the plume will be provided by subglacial flow, although freshwater provided by melt will dominate with sufficient downstream evolution (Jenkins, 2011).

Simple one-dimensional models can provide valuable insights and scaling arguments. Plume theory was initially developed by Morton et al. (1956) to study convection driven by point sources of buoyancy and then applied by Ellison and Turner (1959) in a slightly modified form to the case where buoyancy-driven flow is constrained to follow a solid boundary. MacAyeal (1985) was the first to apply this concept to large-scale circulation beneath ice shelves. According to Jenkins (2011), the main characteristic of all plumes is that their volume flux increases with height by the entrainment of fluid from the surroundings. The approach presented here was used in the work of (Jenkins, 2011). It accounts for all observed melting near the grounding lines. The only difference from previous applications is that the dominant source of buoyancy is defined by the initial conditions rather than the later evolution of the plume. The dynamics of the plume is described by mass, momentum, heat, and salt conservation and considers plume thickness D $[m]$, velocity U $[m \cdot s^{-1}]$, salinity S $[psu]$, where psu is the practical salinity unit, and temperature T $[°C]$ as prognostic variables

$$\frac{d}{dX}(DU) = \dot{e} + \dot{m}, \tag{1}$$

$$\frac{d}{dX}(DU^2) = D\left(\frac{\rho_a - \rho}{\rho_0}\right) g \sin\alpha - C_d U^2, \tag{2}$$

$$\frac{d}{dX}(DUT) = \dot{e}T_a + \dot{m}T_b - C_d^{1/2} U \gamma_T (T - T_b), \tag{3}$$

$$\frac{d}{dX}(DUS) = \dot{e}S_a + \dot{m}T_b - C_d^{1/2} U \gamma_S (S - T_b), \tag{4}$$

where α is the angle of the ice shelf base from the horizontal, $\dot{m}$ $[m \cdot s^{-1}]$ is the melt rate, and the subscripts a indicate conditions in the ambient water and b conditions at the ice–ocean interface (see figure 3). γ_T $[m \cdot s^{-1}]$ and γ_S $[m \cdot s^{-1}]$ is referred as temperature and salinity exchange velocity respectively, $\dot{e}$ is the entrainment rate. C_d is a dimensionless drag coefficient, ρ_a is the ambient water density, ρ_0 $[kg\ m^{-3}]$ is the reference density, and

$$\rho = \rho_0 \left[1 + \beta_S (S - S_a) - \beta_T (T - T_a)\right],$$

describe the equation of the state where β_T is the coefficient of thermal expansion and β_S is the coefficient of haline contraction. The entrainment rate is defined as

$$\dot{e} = E_0 U \sin\alpha,$$

where E_0 is a dimensionless constant. We will discuss the melt rate, and the ice-ocean interface properties further in the following section.

Wells and Worster (2008) also developed a detailed model for a plume rising along a vertical wall, suggesting two transitions. The first from a laminar state to a turbulent regime with a sublayer width set by the Rayleigh number $R_a = g'\delta^3/\kappa\nu$ with $g' = (\rho - \rho_0)g/\rho_0$ where ρ $[kgm^{-3}]$ is the density, g is the gravitational acceleration and δ the molecular sublayer thickness. Then to a second turbulent regime with a sublayer width set by the shear stress of the turbulent external flow, determined by a critical Reynolds number, $R_e = U\delta/\nu$. Despite increasing applications on ocean forcing of glaciers in the past decades, they have not been able to cover the region near the grounding line. For example, the grounding line region, such as in the large vertical Tidewater glaciers of southwest and southeast Greenland, extends 5-10 km from the terminus due to vigorous calving, and the glaciers of northern Greenland, with ice tongues that extend several tens of kilometers. Thus, these studies have failed to sample the ice-ocean boundary layer where the meltwater plume is expected to rise (Straneo et al., 2012). However, it is possible to better understand the dynamics at the ice-ocean boundary by studying the transformation of ocean waters by the glacier in conjunction with thermodynamic models of ice melt in saline waters (Holland and Jenkins, 1999). This approach was recently applied in different studies (e.g. Jenkins (2011); Gayen et al. (2016); Hewitt (2020)).

3 Thermodynamic models of ice-ocean interaction

The aim of modeling the ice-ocean interaction is to obtain a melt rate, interface temperature, and salinity at the ice interface as realistic as possible. To determine the characteristics exactly, three physical constraints have to be considered. The interface must be at the freezing point, heat and salt must be conserved at the interface during any phase change (Holland and Jenkins, 1999).

3.1 Freezing point dependence

The freezing point of seawater is a weakly nonlinear function of salinity and a linear function of pressure (Millero, 1978). However, most studies use a linearized form to simplify the solution to the three-equation system obtained later in this section. The relationship between the temperature and salinity at the ice-ocean interface, T_b $[°C]$ and S_b $[psu]$ is given by

$$T_b = \lambda_1 S_b + \lambda_2 + \lambda_3 p_b \tag{5}$$

where p_b (Pa) is the pressure at the interface and λ_1 $[^\circ C\ psu^{-1}], \lambda_2$ $[^\circ C], \lambda_3$ $[^\circ C Pa^{-1}]$ are constants. Equation (5) is valid only in the salinity range 4-40 psu and does not apply to pure freshwater (Holland and Jenkins, 1999).

3.2 Conservation of heat and salinity

The conservation of heat at the interface requires that the difference of the heat flux balances the source of latent heat resulting from ablation at the interface

$$Q_i^T - Q_a^T = Q_{latent}^T, \tag{6}$$

where $Q_{latent}^T = -\rho_a \dot{m} L_i$ is the latent heat flux with $\rho_a \dot{m}$ representing the mass of ice that melted per unit time. L_i $[Jkg^{-1}]$ is the specific latent heat of the ice. The heat flux at the interface in ice is given by

$$Q_i^T = -\rho_i c_i \kappa_i^T \frac{\partial T_i}{\partial x},$$

and the heat flux at the interface in water is

$$Q_a^T = -\rho_a c_a \kappa_a^T \frac{\partial T_a}{\partial x},$$

where c_i $[J/kg^\circ C], c_a$ $[J/kg^\circ C]$ are the specific heat capacities of ice and ocean; κ_i^T $[m^2 s^{-1}], \kappa_a^T$ $[m^2 s^{-1}]$ are the thermal diffusivities of ice and seawater, and ρ_i is the ice density. The heat conservation at the interface is then

$$\rho_i c_i \kappa_i^T \frac{\partial T_i}{\partial x}\bigg|_b - \rho_a c_a \kappa_a^T \frac{\partial T_a}{\partial x}\bigg|_b = \rho_a \dot{m} L_i. \tag{7}$$

Similarly, the conservation of salinity is given by

$$Q_i^S - Q_a^S = Q_{brine}^S, \tag{8}$$

where $Q_{brine}^S = \rho_a \dot{m}(S_i - S_b)$ is the salt flux necessary to maintain the interface salinity at S_b. The variable Q_i^S represents the diffusive salt flux into the ice, S_i is the salinity in the ice, and the salt flux in the water is

$$Q_a^S = -\rho_a \kappa_a^S \frac{\partial S_a}{\partial x},$$

where κ_a^S is the salinity diffusivity of the seawater. Considering both Q_i^S and S_i negligible (Oerter et al., 1992; Gayen et al., 2016), the salt conservation at the interface becomes

$$\rho_a \kappa_a^s \frac{\partial S_a}{\partial x}\bigg|_b = \rho_a \dot{m} S_b. \tag{9}$$

The equations (7) and (9) represent the boundary conditions at the ice-ocean interface. In some studies, the authors also neglect the heat flux into ice, Q_i^T (eg. Gayen et al. (2016)). The boundary conditions are expressed in terms of melt rate $\dot{m}$, salinity, S_b and temperature, T_b at the boundary, thus we need to compute them in order to solve the boundary equations.

3.3 Three-equation formulation

The three-equation formulation is one of the different approaches used to compute the melt rate, the interface temperature, and salinity. It divides the interface region into ice, the interface of ice-ocean, and the far-field ocean. It describes the conservation of heat equation and salt equation with fluxes across each boundary. This approach was developed by Holland and Jenkins (1999) where the boundary layer is assumed to be laminar. Under this assumption the temperature and salinity would vary linearly between the interface and the mixed temperatures, so we have

$$Q_a^T = -\rho_a c_a \gamma_T (T_b - T_a), \tag{10}$$

and

$$Q_a^S = -\rho_a \gamma_S (S_b - S_a), \tag{11}$$

where γ_T and γ_S are referred to as temperature and salinity exchange velocity respectively. The exchange velocities can be either assumed constant or as function dependence on friction velocity, which we refer to (Holland and Jenkins, 1999) for their parameterization. The temperature gradient for the ice at the ice-ocean interface is given by

$$\left.\frac{\partial T}{\partial x}\right|_b = \frac{\rho_a \dot{m}}{\rho_i \kappa_i^T} \left(T_i - T_b\right). \tag{12}$$

By using the approximation of the heat and salt gradient at the interface, we obtain the three-equation formulation as

$$T_b = \lambda_1 S_b + \lambda_2 + \lambda_3 p_b, \tag{13}$$

$$c_i \dot{m} \left(T_i - T_b\right) + c_a \gamma_T (T_a - T_b) = \dot{m} L_i, \tag{14}$$

$$\gamma_S (S_a - S_b) = \dot{m} S_b. \tag{15}$$

After some algebra, we solve for S_b and find that

$$A S_b^2 + B S_b + C = 0, \tag{16}$$

where

$$\begin{aligned} A &= \lambda_1 (c_a \gamma_T - c_i \gamma_S), \\ B &= -c_a \gamma_T (T_a - \lambda_2 - \lambda_3 p_b) + c_i \gamma_S (T_i - \lambda_2 - \lambda_3 p_b + \lambda_1 S_a) - \gamma_S L_i, \\ C &= \gamma_S L_i S_a - c_i \gamma_S S_a (T_i - \lambda_2 - \lambda_3 p_b). \end{aligned}$$

Although the three-equation formulation is commonly used in recent studies (e.g. Gayen et al. (2016); Gwyther et al. (2020)) to model the oceanic flux at ice-ocean interface, various approaches have been adopted by some other authors. The one-equation formulation described by equation (5) has been used by (eg. Jenkins and Doake (1991); Holland (1998)) and its formulation is based on the fact that if the upper ocean layer relaxes to the freezing point instantaneously, there is no distinction between the properties of the interface and mixed layer. The disadvantage of using this approach come from the fact that the melting rate cannot be computed from the boundary condition. Jenkins et al. (2010) and Jenkins (2011) used, the two-equation formulation define by

$$T_f = \lambda_1 S + \lambda_2 + \lambda_3 p_b \tag{17}$$

$$c_i \dot{m} \left(T_i - T_f\right) + c_a c_d^{1/2} \gamma_{TS} (T_a - T_f) = \dot{m} L_i \tag{18}$$

$$\tag{19}$$

where T_f is the freezing temperature of the plume, and $c_d^{1/2}\gamma_{TS}$ is called Stanton number. Jenkins et al. (2010) shows that the observation of water and melt properties at a Ronne Ice Shelf site can be fitted using either the three-equation or two-equation formulation. One advantage is its use to determine the melting rate.

Now, with the formula of the melt rate, temperature, and salinity at the interface, the boundary conditions, equations (7) and (9) can be rewritten as follows by neglecting the heat flux into ice

$$\left.\frac{\partial T}{\partial x}\right|_b = -\lambda_1 T\Big|_b + \lambda_1 T_a, \quad \lambda_1 = \frac{\gamma_T}{\rho_a \kappa_T}, \tag{20}$$

for the temperature and

$$\left.\frac{\partial S}{\partial x}\right|_b = -\lambda_2 S\Big|_b + \lambda_2 S_a, \quad \lambda_2 = \frac{\gamma_S}{\rho_a \kappa_S}. \tag{21}$$

for salinity. The equations (20) and (21) represent the Robin boundary conditions.

4 Vertical ice face

There have been several studies on quantifying the melt rate in the region dominated by freshwater discharge (Wells and Worster, 2011; Kerr and McConnochie, 2015; Gayen et al., 2016). The melting rate depends not only on the thermal and salt diffusivities but also on the structure of the boundary layer. In the laminar regime, the melting rate is lower due to the thicker thermal boundary layer. At the same time, within the transition region, the interface temperature and melting rate increase rapidly with the rising plume (Gayen et al., 2016). Kerr and McConnochie (2015) in their work considered vertical ice adjacent to the ocean where the melting rate is controlled by the buoyancy-driven dissolving, and it is independent of the depth and plume velocity. They found in their analysis that the melting rate is

$$\dot{m} = k \cdot (T_a - T_f)^{1.34}, \tag{22}$$

where k is constant; this result is consistent with the theory prediction. The authors also pointed out that when the ambient temperature exceeds $3 - 4°C$ above the freezing point temperature, a transition into turbulent melting is approached, and the interface temperature is overestimated. Gayen et al. (2016) solved the Navier-Stokes equations for turbulent flow at a vertical ice-water interface and found good agreement with the experiments of Kerr and McConnochie (2015), consistent with buoyancy controlling the width of the interfacial sublayer. Another theoretical scaling for both vertical and horizontal boundaries suggests the existence of the second regime of turbulent natural convection at high Rayleigh numbers, the numbers associated with the buoyancy-driven flow that characterizes the flow regime ($R_a > 10^{16}$). In that regime, the thickness of the inner laminar boundary layer near the ice face is controlled by shear production rather than convective production of turbulence (Grossmann and Lohse, 2000; Wells and Worster, 2008; Kerr and McConnochie, 2015; Gayen et al., 2016). McConnochie and Kerr (2017) found that for a vertical interface, the transition to a shear regime occurs at a plume speed of 3-5 cm/s. Such small-scale studies provide a unique opportunity to examine the ice-ocean interface and boundary layer development in a controlled environment, which field observations cannot achieve. However, these small-scale studies do not reach the Rayleigh numbers typically observed adjacent to an ice-ocean interface in the field (Malyarenko et al., 2020). Therefore, further studies are needed in the examination of the vertical ice face, glaciers confined to fjords in complex geometries and the Antarctic glacier grounding line region.

5 Numerical Models

Numerical models that include the thermodynamic interaction between the ocean and the ice sheet are the best option for studying current and future Antarctic contributions to sea level (e.g. ROMS:

Dinniman et al. (2007); MITgcm: Losch (2008); FESOM: Timmermann et al. (2012); COCO: Kusahara and Hasumi (2013); MPAS-O: Ringler et al. (2013); FVCOM: Zhou and Hattermann (2020)). MPAS-O was developed based on the finite-volume discretization of the incompressible Boussinesq equations (Ringler et al., 2013).

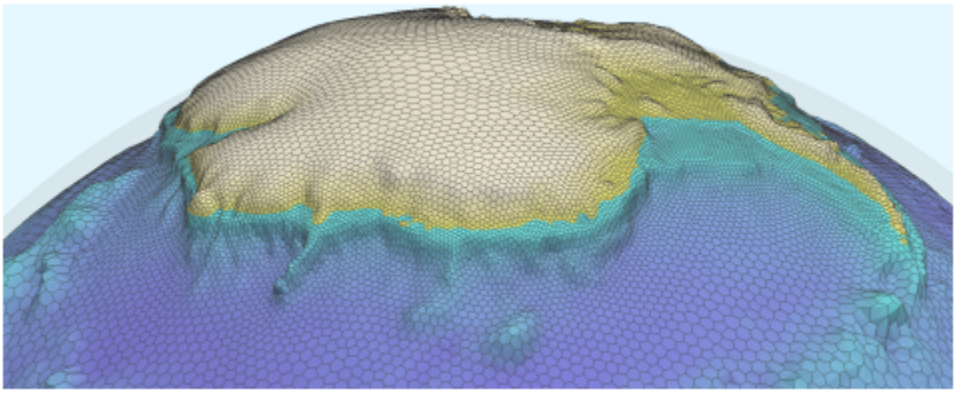

Figure 4: Source (Hoffman and Koch). Example of MPAS grids for the Southern Ocean and Antarctic Ice Sheet.

In MPAS-O, accurate prediction requires acceptable ocean resolution to resolve the currents flowing around or under the ice shelves. Similarly, extremely high resolution, 1 km grid spacing (figure 4) is required to accurately represent the transition between the grounded ice sheet and the floating ice sheet over Antarctica.

Fully coupled ice sheet-ocean models will allow a comprehensive study of how ocean-driven basal melting affects Antarctica, but they are still in their infancy for large realistic domains. Therefore, the best current option is ice shelf-ocean models that neglect ice dynamics and assume steady-state ice geometry (Gwyther et al., 2020). These ice shelf-ocean models explore this data-deficient environment by simulating both small-scale processes and the large-scale spatial and temporal evolution of basal melting in Antarctica. In the recent study done by Gwyther et al. (2020) provides a test case for the development of ice-ocean model applications; and better understanding ice-ocean interactions. The study used three different modeling frameworks, the Regional Ocean Modeling System (ROMS), the Center for Climate System Research Ocean Component Model (COCO), and the Model for Predictions Across Scales: Ocean (MPAS-O).

According to the results of Gwyther et al. (2020), there are significant differences in the basal melting rate between these models, especially with COCO and MPAS compared to ROMS. Melting is lower in ROMS by a factor of two compared to COCO and MPAS-O. In addition, the ROMS model shows lower thermal entrainment (difference between the ambient ocean water temperature T_a and the pressure freezing point T_f) across the ice shelf than COCO and MPAS-O models. According to the authors, the main reason for these results in ROMS is its higher vertical resolution. Their results also suggest a strong sensitivity of melt rates to the choice of vertical resolution, discretization, and boundary layer parameterization that could reasonably affect the sensitivity of the melt rate to changes in ocean forcing. Many authors recognize the limitations of the current treatment of the ice-ocean boundary layer that results in a resolution dependence in melt rates. Gwyther et al. (2020) suggest that until the complete turbulent process can be solved explicitly, parameterizations of processes in the boundary layer will need to evolve with increased vertical resolution.

Understanding the structure and mechanism that governs the thermodynamics and momentum exchange in the ice-ocean boundary layer is limited by the lack of observations and spatial non-uniformity of the ice-ocean interface. Given the non-uniformity of ice-ocean interactions and non-uniform ice melt, the ice face cannot be planar. Therefore, current numerical models developed based on finite difference, finite element, and finite volume methods lack of high-order algorithms and may not provide an

appropriate approximation of the ice-ocean model at the ice face with complex geometry (Figure 4). Thus, the geophysical modeling community is exploring the spectral element method (SEM) approach to address the problems of multi-scale simulations in complex geometrical regions due to the geometric flexibility of their unstructured grids (Iskandarani et al., 2002). It combines the geometric flexibility of low-order finite element methods with the high-order accuracy associated with spectral methods.

According to Iskandarani et al. (2002) and Ilıcak et al. (2009) the SEM method offers several advantages for geophysical simulations such as geometric flexibility with spatial discretization based on unstructured grids, high order convergence rates, dense computations at the element level leading to excellent scalability on parallel computers. Also SEM offers good convergence with the refinement of the elemental grid or increasing the order of the interpolation polynomial and has no significant numerical dissipation (Ilıcak et al., 2009). The figure 5 depicts an example of a spectral element ocean model grid covering the majority of the global ocean. The unstructured grids nature gives the method its great geometrical flexibility and permits a better geometrical description of the complex ocean basins

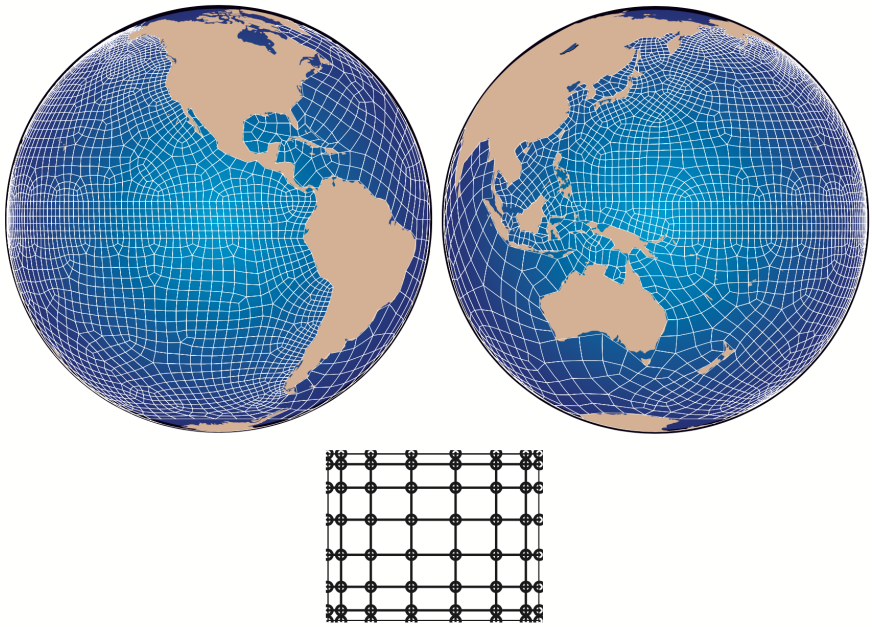

Figure 5: Source (Iskandarani et al. (2002)). Elemental partition of the global ocean as seen from the eastern and western equatorial Pacific. The inset shows the element in the computational domain. The circles mark the interpolation points.

Ilıcak et al. (2009) performed a large eddy simulation (LES) of the lock exchange problem using the non-hydrostatic spectral element model Nek5000. Seven geometric cases with geometric deformations, including V-shaped and L-shaped deformations, which are typically observed in straits, are considered in the simulation. The results revealed significant differences in the amount of mixing between the different domain geometries. In particular, the L-shape leads to the highest level of mixing, and the lowest mixing is encountered in the V-shaped channel. The Nek5000 has also been used in the numerical simulation of bottom gravity currents, and the results have been useful to refine parameterizations of gravity current mixing for an ocean general circulation model (Chang et al., 2005; Ilıcak et al., 2009). From these results, SEM may be helpful to address geometry and high vertical resolution at the ice-ocean interface.

6 Limitations in ice-ocean interaction modeling

According to the papers used in this review, the numerical models have various limitations. Large-scale numerical models have not been able to cover the region near the grounding line, as in the case of the

large vertical tidewater glaciers in Greenland, which extend 5-10 km from the terminus. Thus, without exception, these studies have failed to sample the ice-ocean boundary layer where the meltwater plume is expected to rise (Straneo et al., 2012). Given the topography of the ice face, it will not be realistic to use most of the current models to access this topography. Similarly, it may be unrealistic for large-scale models to resolve plumes of the order of 10 m. Plume models assume a vertical ice front, but actual ice fronts have a more complicated geometry due to non-uniform submarine melt. In addition to the differences between numerical models depending on their framework, ice-ocean models, in general, are still subject to several limitations. Some of these are related to significant uncertainties in the ice face geometry and critical gaps in the knowledge of the dynamics at the ice-ocean interface, as Mathiot et al. (2017) highlighted in the case of the Nucleus for European Modeling of the Ocean (NEMO) framework.

Improved predictions of the contribution of the glaciers, ice sheets, and sea ice melt to sea level rise require a better understanding of the processes that influence ice dynamics. The three-equation formulation that describes the thermodynamics of the ice-ocean interface assumes only vertical flows with no horizontal flows. However, Jenkins (2016) shows that an equilibrium state could be reached only in the boundary layer with a sloping interface and a buoyant plume if spatial gradients were present in properties such as temperature or horizontal velocity. The three-equation formulation has been applied to many ice-ocean models with different vertical configurations. The practical implementation of these parameterizations differs among model settings; thus, the results of ice-ocean simulations with different models may treat this vertical resolution dependence differently (Gwyther et al., 2020). Although the three-equation formulation has been used in many models and studies to quantify melt rate, observations of double diffusive staircases under the George VI ice shelf (Kimura et al., 2015) are an illustration where it has been shown that the three-equation formulation does not accurately resolve melt rate. Davis and Nicholls (2019) showed that the wall law assumption inherent in the three-equation formulation does not hold at low flow rates.

7 Future Research Ideas

From the previous sections, we noticed that the current models for ice-ocean interaction have a limit in capturing the ice interface well, the plume, and the three-equation formulation's failure in the double-diffusivity situation and low flow rate. Therefore, additional studies are needed and may focus on:

- Understand the physics and processes that govern heat and salt transfer from the ocean outside the boundary layer to the ice face. Consider better parameterization of critical processes (e.g., basal melting) in the ice-ocean interaction and their better integration into numerical models. Consider an improved model resolution to capture the plume at the interface well.

- In the three-equation formulation, the boundary values, temperature, and salinity are known, making the problem of Dirichlet conditions. However, given the non-uniform melting of the ice face and the plume dynamics in the boundary layer, which must rise from the bottom to the top of the ice, it may be appropriate to prescribe boundary conditions like Neumann or Robin.

- Given the non-stationary state of the flow near the ice-ocean interface, it may also be worthwhile to improve the three-equation formulation and include the properties of horizontal flows.

- In recent years, some ice-ocean interaction studies have applied numerical models based on the spectral method. However, it is not yet as widespread as finite difference and finite volume method models. Therefore, numerical ice-ocean interaction models based on the spectral element method or the discontinuous Galerkin (DG) method could be developed, as these methods can help solve the geometric complexity of the ice face. In the DG method, the numerical solution can be discontinuous across element boundaries. The fluxes do the communication between the elements exchanged across the edges of the elements.

References

M. Bersch, I. Yashayaev, and K. P. Koltermann. Recent changes of the thermohaline circulation in the subpolar North Atlantic. *Ocean Dynamics*, 57(3):223–235, 2007.

J. E. Box, L. Yang, D. H. Bromwich, and L.-S. Bai. Greenland ice sheet surface air temperature variability: 1840–2007. *Journal of Climate*, 22(14):4029–4049, 2009.

G. Catania, L. Stearns, T. Moon, E. Enderlin, and R. Jackson. Future evolution of Greenland's marine-terminating outlet glaciers. *Journal of Geophysical Research: Earth Surface*, 125(2):e2018JF004873, 2020.

Y. S. Chang, X. Xu, T. M. Özgökmen, E. P. Chassignet, H. Peters, and P. F. Fischer. Comparison of gravity current mixing parameterizations and calibration using a high-resolution 3D nonhydrostatic spectral element model. *Ocean Modelling*, 10(3-4):342–368, 2005.

P. E. Davis and K. W. Nicholls. Turbulence observations beneath Larsen C ice shelf, Antarctica. *Journal of Geophysical Research: Oceans*, 124(8):5529–5550, 2019.

R. M. DeConto and D. Pollard. Contribution of Antarctica to past and future sea-level rise. *Nature*, 531(7596):591–597, 2016.

M. S. Dinniman, J. M. Klinck, and W. O. Smith Jr. Influence of sea ice cover and icebergs on circulation and water mass formation in a numerical circulation model of the Ross Sea, Antarctica. *Journal of Geophysical Research: Oceans*, 112(C11), 2007.

B. Gayen, R. W. Griffiths, and R. C. Kerr. Simulation of convection at a vertical ice face dissolving into saline water. *Journal of Fluid Mechanics*, 798:284–298, 2016.

S. Grossmann and D. Lohse. Scaling in thermal convection: a unifying theory. *Journal of Fluid Mechanics*, 407:27–56, 2000.

D. E. Gwyther, K. Kusahara, X. S. Asay-Davis, M. S. Dinniman, and B. K. Galton-Fenzi. Vertical processes and resolution impact ice shelf basal melting: A multi-model study. *Ocean Modelling*, 147: 101569, 2020.

I. J. Hewitt. Subglacial plumes. *Annual Review of Fluid Mechanics*, 52:145–169, 2020.

M. Hoffman and D. Koch. The model for prediction across scales framework: A flexible foundation for next-generation earth system model components. `https://e3sm.org/wp-content/uploads/2018/03/ResearchHighlight_ModelPrediction_V5.pdf`. Accessed: 2021-10-24.

D. M. Holland. On the parameterization of basal heat flux for sea-ice modeling. *Geophysica*, 34(1-2): 1–21, 1998.

D. M. Holland and A. Jenkins. Modeling thermodynamic ice–ocean interactions at the base of an ice shelf. *Journal of Physical Oceanography*, 29(8):1787–1800, 1999.

M. Ilıcak, T. M. Özgökmen, E. Özsoy, and P. F. Fischer. Non-hydrostatic modeling of exchange flows across complex geometries. *Ocean Modelling*, 29(3):159–175, 2009.

M. Iskandarani, D. B. Haidvogel, J. C. Levin, E. Curchitser, and C. A. Edwards. Multi-scale geophysical modeling using the spectral element method. *Computing in Science & Engineering*, 4(5):42–48, 2002.

A. Jenkins. Convection-driven melting near the grounding lines of ice shelves and tidewater glaciers. *Journal of Physical Oceanography*, 41(12):2279–2294, 2011.

A. Jenkins. A simple model of the ice shelf–ocean boundary layer and current. *Journal of Physical Oceanography*, 46(6):1785–1803, 2016.

A. Jenkins and C. Doake. Ice-ocean interaction on Ronne Ice Shelf, Antarctica. *Journal of Geophysical Research: Oceans*, 96(C1):791–813, 1991.

A. Jenkins and D. M. Holland. A model study of ocean circulation beneath Filchner-Ronne Ice Shelf, Antarctica: Implications for bottom water formation. *Geophysical research letters*, 29(8):34–1, 2002.

A. Jenkins, K. W. Nicholls, and H. F. Corr. Observation and parameterization of ablation at the base of Ronne Ice Shelf, Antarctica. *Journal of Physical Oceanography*, 40(10):2298–2312, 2010.

I. Joughin, R. B. Alley, and D. M. Holland. Ice-sheet response to oceanic forcing. *Science*, 338(6111): 1172–1176, 2012.

R. C. Kerr and C. D. McConnochie. Dissolution of a vertical solid surface by turbulent compositional convection. *Journal of Fluid Mechanics*, 765:211–228, 2015.

S. Kimura, K. W. Nicholls, and E. Venables. Estimation of ice shelf melt rate in the presence of a thermohaline staircase. *Journal of Physical Oceanography*, 45(1):133–148, 2015.

K. Kusahara and H. Hasumi. Modeling Antarctic ice shelf responses to future climate changes and impacts on the ocean. *Journal of Geophysical Research: Oceans*, 118(5):2454–2475, 2013.

M. Losch. Modeling ice shelf cavities in az coordinate ocean general circulation model. *Journal of Geophysical Research: Oceans*, 113(C8), 2008.

A. Malyarenko, A. J. Wells, P. J. Langhorne, N. J. Robinson, M. J. Williams, and K. W. Nicholls. A synthesis of thermodynamic ablation at ice-ocean interfaces from theory, observations and models. *Ocean Modelling*, page 101692, 2020.

P. Mathiot, A. Jenkins, C. Harris, and G. Madec. Explicit representation and parametrised impacts of under ice shelf seas in the z coordinate ocean model NEMO 3.6. *Geoscientific Model Development*, 10 (7):2849–2874, 2017.

C. D. McConnochie and R. C. Kerr. Using Laboratory Experiments to Improve Ice-Ocean Parameterizations. In *AGU Fall Meeting Abstracts*, volume 2017, pages C23A–1210, 2017.

F. Millero. Freezing point of sea water. *eighth report of the Joint Panel of Oceanographic Tables and Standards, appendix*, 6:29–31, 1978.

R. J. Motyka, L. Hunter, K. A. Echelmeyer, and C. Connor. Submarine melting at the terminus of a temperate tidewater glacier, LeConte Glacier, Alaska, USA. *Annals of Glaciology*, 36:57–65, 2003.

F. M. Nick, A. Vieli, I. M. Howat, and I. Joughin. Large-scale changes in Greenland outlet glacier dynamics triggered at the terminus. *Nature Geoscience*, 2(2):110–114, 2009.

F. M. Nick, A. Vieli, M. L. Andersen, I. Joughin, A. Payne, T. L. Edwards, F. Pattyn, and R. S. Van De Wal. Future sea-level rise from Greenland's main outlet glaciers in a warming climate. *Nature*, 497(7448):235–238, 2013.

T. Noble, E. Rohling, A. R. A. Aitken, H. C. Bostock, Z. Chase, N. Gomez, L. M. Jong, M. A. King, A. N. Mackintosh, F. McCormack, et al. The sensitivity of the Antarctic ice sheet to a changing climate: past, present, and future. *Reviews of Geophysics*, 58(4):e2019RG000663, 2020.

H. Oerter, J. Kipfstuhl, J. Determann, H. Miller, D. Wagenbach, A. Minikin, and W. Graft. Evidence for basal marine ice in the Filchner–Ronne Ice Shelf. *Nature*, 358(6385):399–401, 1992.

E. Rignot and S. S. Jacobs. Rapid bottom melting widespread near Antarctic ice sheet grounding lines. *Science*, 296(5575):2020–2023, 2002.

E. Rignot, M. Koppes, and I. Velicogna. Rapid submarine melting of the calving faces of West Greenland glaciers. *Nature Geoscience*, 3(3):187–191, 2010.

T. Ringler, M. Petersen, R. L. Higdon, D. Jacobsen, P. W. Jones, and M. Maltrud. A multi-resolution approach to global ocean modeling. *Ocean Modelling*, 69:211–232, 2013.

J. Schaffer, W.-J. von Appen, P. A. Dodd, C. Hofstede, C. Mayer, L. de Steur, and T. Kanzow. Warm water pathways toward Nioghalvfjerdsfjorden Glacier, Northeast Greenland. *Journal of Geophysical Research: Oceans*, 122(5):4004–4020, 2017.

F. Straneo and C. Cenedese. The dynamics of Greenland's glacial fjords and their role in climate. *Annual review of marine science*, 7:89–112, 2015.

F. Straneo and P. Heimbach. North Atlantic warming and the retreat of Greenland's outlet glaciers. *Nature*, 504(7478):36–43, 2013.

F. Straneo, D. A. Sutherland, D. Holland, C. Gladish, G. S. Hamilton, H. L. Johnson, E. Rignot, Y. Xu, and M. Koppes. Characteristics of ocean waters reaching Greenland's glaciers. *Annals of Glaciology*, 53(60):202–210, 2012.

F. Straneo, P. Heimbach, O. Sergienko, G. Hamilton, G. Catania, S. Griffies, R. Hallberg, A. Jenkins, I. Joughin, R. Motyka, et al. Challenges to understanding the dynamic response of greenland's marine terminating glaciers to oceanic and atmospheric forcing. *Bulletin of the American Meteorological Society*, 94(8):1131–1144, 2013.

R. Timmermann, Q. Wang, and H. Hellmer. Ice-shelf basal melting in a global finite-element sea-ice/ice-shelf/ocean model. *Annals of Glaciology*, 53(60):303–314, 2012.

M. van den Broeke, J. Bamber, J. Ettema, E. Rignot, E. Schrama, W. J. van de Berg, E. van Meijgaard, I. Velicogna, and B. Wouters. Partitioning recent Greenland mass loss. *Science*, 326(5955):984–986, 2009.

J. Weertman. Stability of the junction of an ice sheet and an ice shelf. *Journal of Glaciology*, 13(67): 3–11, 1974.

A. J. Wells and M. G. Worster. A geophysical-scale model of vertical natural convection boundary layers. *Journal of Fluid Mechanics*, 609:111–137, 2008.

A. J. Wells and M. G. Worster. Melting and dissolving of a vertical solid surface with laminar compositional convection. *Journal of fluid mechanics*, 687:118–140, 2011.

Q. Zhou and T. Hattermann. Modeling ice shelf cavities in the unstructured-grid, Finite Volume Community Ocean Model: Implementation and effects of resolving small-scale topography. *Ocean Modelling*, 146:101536, 2020.